Int. J. Environ. Sci. Technol. (2018) 15:863–874
https://doi.org/10.1007/s13762-017-1446-4

ORIGINAL PAPER

Preparation of magnetic microgels for catalytic reduction of 4-nitrophenol and removal of methylene blue from aqueous medium

F. Bibi[1] · M. Ajmal[2] · F. Naseer[1] · Z. H. Farooqi[3] · M. Siddiq[1]

Received: 16 October 2016 / Revised: 24 January 2017 / Accepted: 15 July 2017 / Published online: 26 July 2017

Abstract This work describes the synthesis of poly(acrylic acid) microgels and fabrication of magnetic cobalt nanoparticles in the prepared microgels. Cobalt nanoparticles were fabricated by loading the cobalt (II) ions in microgels from aqueous solution and their subsequent reduction with sodium borohydride ($NaBH_4$). Bare and composite microgels were characterized by Fourier transform infrared spectroscopy, scanning electron microscopy and transmission electron microscopy. The catalytic properties of the prepared microgel composites were investigated by using them as catalyst for the reduction of 4-nitrophenol and methylene blue. The effect of temperature and catalyst dose on the rate of reduction of these toxic pollutants was investigated. The reusability of prepared catalysts was also studied for the five consecutive cycles, and an increase in catalytic activity was observed after every cycle. The prepared bare and magnetic microgels were found as very effective adsorbent for the removal of methylene blue from aqueous medium. Very rapid adsorption rate was found for the removal of methylene as its 100 mg was adsorbed on per gram of dried hydrogels in about 25 min. The effects of different parameters like amount of adsorbate and concentration of adsorbent on the adsorption process were studied. Langmuir, Freundlich and Temkin adsorption isotherms were applied, and it was found that adsorption of MB follows Freundlich model better than others. Furthermore, pseudo-first-order and pseudo-second-order kinetic models were also applied and adsorption of MB was found to abide by pseudo-second-order kinetics.

Keywords Microgels · Nanoparticles · Catalysis · Adsorption · Pollutants

Introduction

Every type of pollution or sources of contamination have their own devastation on animals, plants and eventually on human beings. The heavy metals contamination in water is one of the severe concerns which may be due to their carcinogenic nature and non-biodegradability. Along with heavy metals contamination, organic dyes which are released from textile, plastic, cosmetic and paper industries are also the major sources of water contaminants. The occurrence of these toxic dyes explicitly in the aquatic system can cause some severe diseases such as quadriplegia, vomiting, cyanosis, tissue necrosis, jaundice, increase in heartbeat and shock (Mak and Chen 2004; Zendehdel et al. 2010). Certain dyes and their associated degradation products are also highly toxic, noxious and have carcinogenic effect on human health. So, in order to protect our environment from harmful effects of heavy metals and toxic organic dyes, their elimination from waters has become a subject of universal attention (Yagub et al. 2014; Ahmad et al. 2010). One of the most commonly used methods for cleaning of water is adsorption of toxic water pollutants by using

Editorial responsibility: M. Abbaspour.

Electronic supplementary material The online version of this article (doi:10.1007/s13762-017-1446-4) contains supplementary material, which is available to authorized users.

✉ M. Siddiq
m_sidiq12@yahoo.com

[1] Department of Chemistry, Quaid-i-Azam University, Islamabad 45320, Pakistan

[2] Institute of Chemical Sciences, Bahauddin Zakariya University, Multan 60800, Pakistan

[3] Institute of Chemistry, University of the Punjab, New Campus, Lahore, Pakistan

appropriate sorbents. For example, acrylonitrile resin has been used as adsorbents by de Santa Maria et al. (2001) for the removal of the heavy metals from water. Similarly, Yang et al. (2011) reported graphene oxide as adsorbent for the removal of methylene blue and rhodamine 6G from aquatic environment. Hydrogels are becoming more popular as compared to other adsorbents in order to remove the water toxins and contaminants. Due to the presence of hydrophilic groups and their cross-linking nature, hydrogels show size variation with change in the external stimuli. For example, temperature, ionic strength of the solution and pH of the selected medium cause swelling in volume of the hydrogels as compared to the original volume of the hydrogel in dry form (Hernández and Mijangos 2009). Hydrogels have gained much interest due to the hydrophilic functional groups such as –COOH, –OH, $–NH_2$, $–CONH_2$, $–SO_3H$ (Ozay et al. 2010). Also, due to their effortless handling, biocompatibility, environmental friendly nature and their associated reusability for the development of effective desorption process, the hydrogels have become very useful materials for the removal of heavy metals, herbicides and organic dyes and many other pollutants from aqueous medium. In addition to these pollutants, nitro aromatic compounds released from industries are the other considerable source of pollutants. 4-Nitrophenol (4-NP) is one of the major refractory pollutants that are found in agriculture and industrial effluents as they are soluble and stable for a long time in water. Because of their harmful nature, the US Environmental Protection Agency (EPA) has listed nitrophenols as pollutant materials (Shaoqing et al. 2010). They have also been reported for poisoning aquatic life and causing odor problems in water reservoirs (Megharaj et al. 1991). Therefore, for environmental protection, their removal from industrial effluents has vital significance (Dai et al. 2009). In addition, catalytic reduction of the nitro aromatic compounds into the amines is an important process that is mostly used in synthetic organic chemistry and also in the synthesis of various important industrial products; for example, functionalized anilines have great industrial importance because they are used as a reactive intermediate for photographic, pharmaceutical and also in plastic industries (Mak and Chen 2004; Sahiner et al. 2010a, b).

Hydrogels containing metal nanoparticles have been proved as effective catalysts for the reduction of nitro compounds. Due to their soft and flexible nature, hydrogels provide a controlled reaction medium. On the other hand, the chemical nature and cross-linking of network prevent the aggregation of metal nanoparticles which actually act as catalysts. Due to this dual action, i.e., providing a reaction medium and acting as a catalyst, hydrogels fabricated with catalytically active metal nanoparticles have become very popular catalysts for the reactions in aquatic medium. For example, Sahiner et al. (2010a, b) reported the fabrication of cobalt nanoparticles in soft hydrogel reactor and the prepared composites were used as catalyst for reduction of 2-nitrophenol (2-NP) and 4-NP. The hydrogels were found to be able to prevent the aggregation as well as the oxidation of nanoparticles which was demonstrated by the shelf life, and after five days of storage time, only 1% loss in catalytic activity was observed. Ajmal et al. (2014) employed poly(-methacrylic acid) (p(MAc)) microgels as a template for the preparation of Cu, Ni and Co nanoparticle and found these composites as effective catalysts for reduction of organic aromatic dyes and aromatic nitro compounds from aqueous solutions. Similarly, Ozay et al. (2011) prepared Co, Cu and Ni nanoparticles inside hydrogel networks of 2-acrylamido-2-methyl-1-propansulfonic acid (AMPS) and used them as catalyst in the generation of hydrogen by hydrolysis of ammonia borane. Khan et al. (2011) employed poly(NIPAM-co-AAc) hydrogel network for in situ fabrication of silver nanoparticles and used as catalyst. Another big advantage of using hydrogels–metal nanoparticle composites as catalysts is that they can be easily recovered from the reaction medium after completing their catalytic role. Furthermore, magnetic metal nanoparticles can be prepared inside the hydrogels resulting in the formation of magnetic hydrogel–metal nanoparticles which can be more easily removed from reaction mixture by applying an external magnetic field. Ozay et al. (2009) prepared magnetic hydrogels and used them as adsorbents for the elimination of toxic heavy metal ions from aqueous medium. In this study, it was demonstrated that after adsorption the hydrogel retained their magnetic character and can be removed from the reaction medium by applying external magnetic field. Ozay et al. (2010) also synthesized magnetic hydrogels by incorporating iron oxide nanoparticles in poly(2-acrylamido-2-methyl-1-propansulfonic acid-co-vinylimidazole) (p(AMPS-co-VI)) hydrogel network and employed as adsorbents for the removal of toxic metal ions from aquatic environment. Similarly, Ajmal et al. (2015a, b) used microgels for the synthesis of coblat–iron bimetallic magnetic nanoparticles. These microgel systems were also found to retain their magnetic properties after the adsorption of heavy metal ions, organic dyes and herbicides from water.

Here, we reported the synthesis p(AAc) microgels and fabrication of inherently magnetic cobalt nanoparticles inside the microgel network by in situ reduction of Co (II) ions. The prepared microgels were used as adsorbent for the removal of industrial dye MB and as catalyst for the reduction of 4-NP. The effects of different parameters such as amounts of adsorbents or catalysts, amounts of adsorbate and temperature of the reaction medium were also studied for both the adsorption and catalytic applications.

Date and location of research: 2016, Quaid-i-Azam University, Islamabad, Pakistan.

Materials and methods

Materials

Acrylic acid (AAc, 99%, Alfa Aesar) was used as monomer, *N*,*N*-methylenebisacrylamide (MBA, 99%, Sigma Aldrich) as the cross-linking agent, *N*,*N*,*N*′,*N*′-tetramethylethylenediamine (TEMED, 99% Merck) as an accelerator and ammonium persulfate (APS 98%, Sigma Aldrich) as initiator. The cyclohexane (99.5%, DAEJUNG KOSDAQ) was used as solvent, and the surfactant sorbitan monooleate Span 80 (AVONCHEM) was used as stabilizer. We used NaOH (98%, Aldrich) for neutralization of poly(AAc) microgels. Cobalt (II) nitrate ($CoNO_3$) was used as a source for Co (II) ions. Sodium borohydride ($NaBH_4$, 98%, Merck) was used as reducing agent. 4-Nitrophenol (4-NP, 99% Aldrich) was used as a nitro organic pollutant. Methylene blue (MB, DC Panreac) was used as organic dye. Deionized (DI) water was used to carry out all the experimental work of this study.

Synthesis of poly(acrylic acid) p(AAc) microgels

The p(AAc) microgels were synthesized through inverse suspension polymerization. A 50 mL cyclohexane was taken in 100-mL round-bottomed flask containing 200 μL sorbitan monooleate Span 80, and this mixture was stirred to homogenize and heated to 40 °C. This mixture was also purged with N_2 gas for 15 min to remove oxygen. The polymerization and cross-linking reaction was carried out by mixing 0.133 g APS (2 mol% of AAc) dissolved in 1 mL DI water, 0.045 g MBA (1 mol% of AAc) dissolved in 1 mL DI water and 2 mL acrylic acid in a glass vial. Then, this mixture was homogenized by shaking and added into flask which was already containing cyclohexane and sorbitan Span 80. To remove oxygen, this reaction was purged with N_2 for further 10 min. Then, 250 μL TEMED, the accelerator, was added in reaction mixture and the formation of microgel particles was started within 5 min of the addition of TEMED. The reaction was allowed to proceed for further 4 h. At the end of reaction, the microgel particles were collected by decantation of solvent. In order to remove the unreacted species and impurities, microgels were washed by using acetone and DI water for at least five times. After cleansing, the microgel particles were neutralized. For this purpose, the prepared p(AAc) microgel was treated with excess amount (threefold excess number of moles) of NaOH for overnight. The microgels were washed again with excess amount of DI water and acetone for at least three times. Finally, p(AAc) microgel particles were dried in oven at 60 °C.

Synthesis of p(AAc)-Co composites

P(AAc)-Co microgel composites were synthesized by in situ fabrication of magnetic Co nanoparticles. For in situ synthesis of cobalt nanoparticles in the microgel network, firstly the cobalt (II) ions were loaded by adding 0.5 g of dried and neutralized p(AAc) microgels into 250 mL and 500 ppm aqueous solution of cobalt nitrate and kept it at continuous stirring for 2 h. The metal ions were loaded in microgels, and color of the microgels was turned to pink. The metal ion-loaded microgels were then filtered through plankton cloth filter paper (2 μm pore size) and washed with DI water three times to get rid of impurities and unbound metal ions. Finally, these metal ion laden microgel particles were dried in oven at 60 °C for drying. After drying, the pink color laden microgel particles were changed to plum color. To carryout reduction of metal ions inside the microgel network, these laden microgel particles were treated with $NaBH_4$ (50 mL, 0.1 M) solution. The reduction reaction was preceded till all H_2 gas was evolved. These microgel composites were then filtered through plankton cloth filter. Finally, washing was carried out with DI water. These composites were then used for characterization and applications.

Catalytic experiments

Prepared composites (p(AAc)–Co) were used as a catalyst for the reduction of nitro aromatic compound and industrial dye, i.e., 4-NP and MB, respectively. A 50 mL solution of 1 mM 4-NP was prepared, and to this solution 50 mg composite microgel was added as a catalyst and the reaction was allowed to take place in a flask which was adjusted in temperature-controlled silicon oil bath to maintain the desirable temperature. To this mixture, 0.19 g $NaBH_4$ was added for initiation of reduction reaction. During the reaction, 0.3 mL sample was taken from the reaction mixture and diluted with deionized water. The progress of reaction was monitored by UV–Visible spectrophotometer (Shimadzu 1601). Reduction rate constants for 4-NP were measured from the gradual decrease in absorbance peak at 400 nm. The effect of catalyst dose was studied by taking four different amounts (0.01, 0.05, 0.10 and 0.15 g) of p(AAc)-Co catalyst and keeping all other reaction parameters constant. Similarly, four different temperatures, i.e., 30, 40, 50 and 60 °C, were selected to study the effect of temperature on the rate of reaction. The reusability of composites was also studied. To carry out reusability, after each cycle the p(AAc)-Co catalysts were separated from the reaction medium, washed with DI water and used again for same reaction under same conditions. Catalytic activity of p(AAc)-Co was also investigated for the reduction of MB. In a typical experiment, 30 mg of $NaBH_4$ was used as reducing agent for 50 mL of 1.6×10^{-4} M MB solution. 0.5 mL sample was taken from the reaction

medium and diluted with deionized water. The progress of reaction was monitored by UV–Visible spectrophotometer (Shimadzu 1601).

Adsorption experiments

Adsorption experiments were conducted at room temperature. A 100 mL, 1.6×10^{-4} M (5.118 ppm) solution of methylene blue (MB) was taken in separate beaker. In MB solution, 50-mg microgel particles were added. This solution was then stirred at 400 rpm. After specific time interval, 0.5-mL sample was taken from reaction mixture and diluted with DI water. UV–Vis spectrophotometer (Shimadzu 1601) was used to monitor the amount of MB dye adsorbed. In order to study the effect of amount of adsorbent, different amounts of microgels, i.e., 12.5, 25.0, 50.0 and 75.0 mg, were used to adsorb MB dye from 1.6×10^{-4} M, 100 mL MB solution. Furthermore, the effect of the initial concentration of MB solution on adsorption capacity of pure microgels was studied. For this purpose, MB solutions of different concentrations, i.e., 0.8×10^{-4}, 1.6×10^{-4}, 2.4×10^{-4} and 3.2×10^{-4} M (2.558, 5.118, 7.676 and 10.235 ppm), were prepared while keeping the amount of microgels same, i.e., 50 mg. The adsorption process was carried out at room temperature and 400 rpm. After specific intervals of time, 0.5-mL sample was withdrawn, and after proper dilution with DI water the adsorption was monitored by UV–Visible spectrophotometer by measuring concentration of MB in terms of absorbance at $\lambda_{max} = 664$ nm.

Characterization

The FT-IR spectra of microgels and their composite were recorded with Fourier transforms infrared spectrometer (RX I FT-IR spectrophotometer, PerkinElmer, USA). Shimadzu 1601 UV–Visible spectrophotometer was used to investigate the adsorption and catalytic property of pure and composite materials. The morphology and size of pure microgels were studied by (TESCAN, MIRA3) scanning electron microscope (about 10 kV accelerating voltage). Transmission electron microscope (TEM, JEOL 2010, Japan) was used to visualize the metal nanoparticles in microgel network.

Results and discussion

Synthesis of poly(acrylic acid) p(AAc) microgels

The p(AAc) microgels were synthesized by inverse suspension polymerization as previously described in experimental part. Monodispersed microgels were formed by the reaction of monomer (AAc), initiator (APS) and cross-linker (MBA). TEMED was also used, which acted as accelerator. Polymerization was started by initiator which reacted with monomers, and oligomers were formed. The combination of oligomers with other oligomers or monomers resulted in the formation of stable microgel particles. The surface morphology and size of pure microgels were studied by SEM. The SEM image of pure p(AAc) microgels is shown in Fig. 1a, which indicates that well-defined spherical microgel particles were obtained without forming any aggregation and most of the particles have diameter around 50 nm.

Synthesis of p(AAc)-Co composites

The p(AAc)-Co microgel composites were synthesized by in situ fabrication of magnetic Co nanoparticles. The schematic representation for the fabrication of metal nanoparticles in p(AAc)-Co microgel is illustrated in Fig. 1b.

For in situ synthesis, firstly the cobalt (II) ions were loaded in p(AAc) microgels from the aqueous solution of cobalt nitrate. The p(AAc) microgel contains carboxyl groups which are deprotonated upon reacting with NaOH and become negatively charged. These negatively charged groups attract positively charged Co (II) ions. The force of attraction between negatively charged carboxyl groups and positively charged Co (II) ions acts as bond between them. Due to the presence of this bond, the metal ions which are entrapped in microgel cannot leave the network. The $NaBH_4$ is a reducing agent, and when metal ions loaded microgel is treated with $NaBH_4$. The metal ions are reduced and form metal nanoparticles. The physical appearance of the reaction mixture is also shown with digital camera images. The image 1 represents the bare p(AAc) microgel which shows that bare microgel possesses light yellow color. After absorption of Co (II) ions, the microgel attains pink color as shown in image 2. The pink coloration of microgel indicates that Co (II) ions were loaded in microgel. The color of microgels is turned to black after the formation of nanoparticles as shown in image 3. The cobalt nanoparticles have black color so the blackening of microgel indicates the formation of Co nanoparticles in microgel. TEM was used to confirm and visualize the formation and presence of metal nanoparticles in microgel network and also to know about its morphology, size and shape. Figure 1c shows the TEM image of Co nanoparticles fabricated in p(AAc) microgels. The TEM image reveals that the nanoparticles were evenly distributed and show no aggregation. The absence of aggregation reveals the stability of Co nanoparticles in microgel network.

The magnetic property of the prepared p(AAc)-Co composites can be seen from the digital camera images in

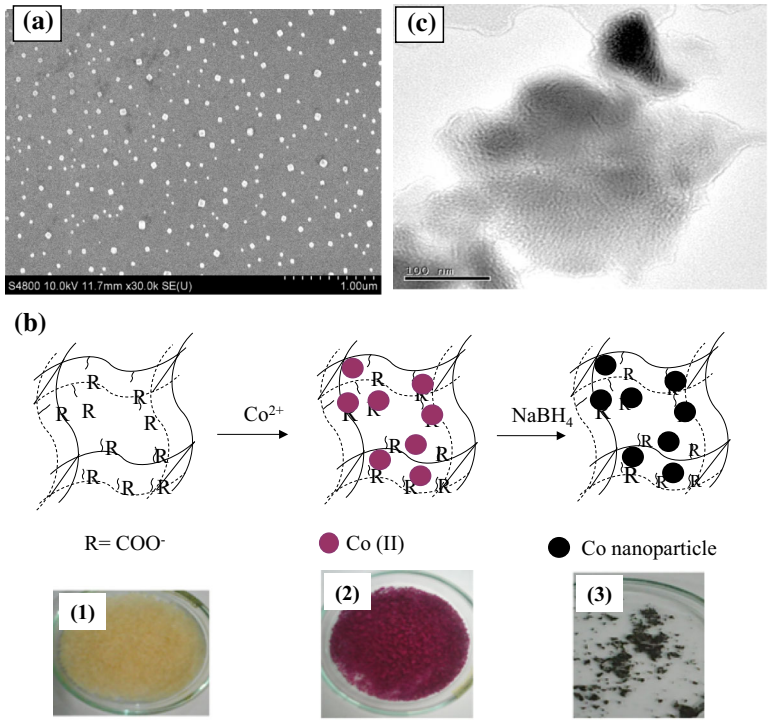

Fig. 1 **a** SEM image of p(AAc) microgel particles. **b** TEM image of cobalt nanoparticles prepared in p(AAc) microgels. **c** The schematic representation of in situ fabrication of Co nanoparticles in p(AAc) hydrogel network and their corresponding digital camera images

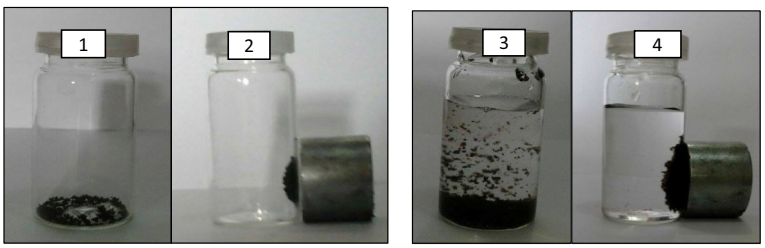

Fig. 2 Digital camera images of p(AAc)-Co composites. Dried p(AAc)-Co composites (**1**) in the absence and (**2**) in the presence of external magnetic field. P(AAc)-Co composites suspended in water (**3**) in the absence and (**4**) in the presence of external magnetic field

Fig. 2. The image 1 represents the dried p(AAc)-Co microgel composites in the absence of external magnetic field. The image 2 shows that dried p(AAc)-Co composites were attracted toward externally applied magnetic field. The camera image 3 represents the p(AAc)-Co microgel in suspended in water, and the image 4 shows the attraction of p(AAc)-Co microgel form water to the magnet. The movement of microgel–metal nanoparticle composites toward magnet confirms that these composites possess magnetic characteristics. This magnetic behavior of microgel–metal nanoparticle composites provided a very simple and easy way of their separation from the reaction mixture that is the application of external magnetic field. Nowadays, a lot of attention is given to such type of novel adsorbents and catalysts that can be easily separated from the reaction mixture or from solutions to make its applicability in daily life. That's why magnetic hydrogels have gained much interest for water purification as its separation is easier than many other materials having no magnetic responsive behavior.

The FT-IR was used to confirm and identify different functional groups which were present in the microgels. The FT-IR spectra of pure p(AAc) and composite p(AAc)-Co microgel are shown in Fig. S2. The FT-IR spectra show characteristic peaks at different positions for different functional groups. For bare p(AAc) microgel particles, the peak at 2920 cm^{-1} was ascribed to the aliphatic C–H anti symmetric stretching, the peak at 1700 cm^{-1} was attributed to the acid C=O stretching, and the peak at 1316 cm^{-1} was due to acid C–O stretching. The peak at 1655 cm^{-1} represents the amide C=O stretching, and the amide N–H stretching is present at about 3346 cm^{-1}. All of these are characteristics peaks for p(AAc) microgels. In the case of the p(AAc)-Co composite, the peaks of acid C=O stretching, amide C=O stretching and the amide N–H stretching are present at 1650, 1540 and 3250 cm^{-1}, respectively. It was observed that all these peaks

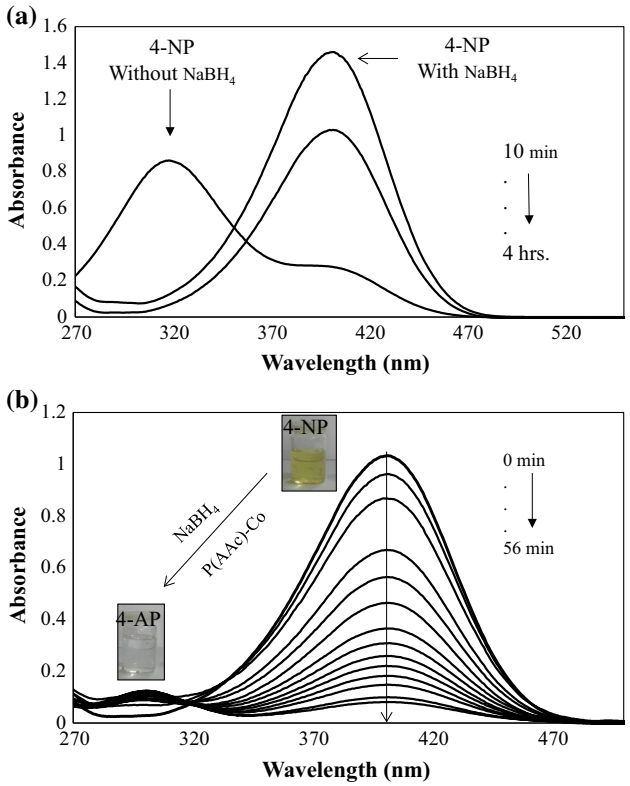

Fig. 3 UV–visible spectra for the reduction of 4-NP by $NaBH_4$ **(a)** in the absence of p(AAc)-Co catalyst. **b** In the presence of p(AAc)-Co catalyst. Reaction conditions: 1 mM 4-NP = 50 mL, catalyst = 50 mg, $NaBH_4$ = 0.19 g, 250 rpm and 30 °C

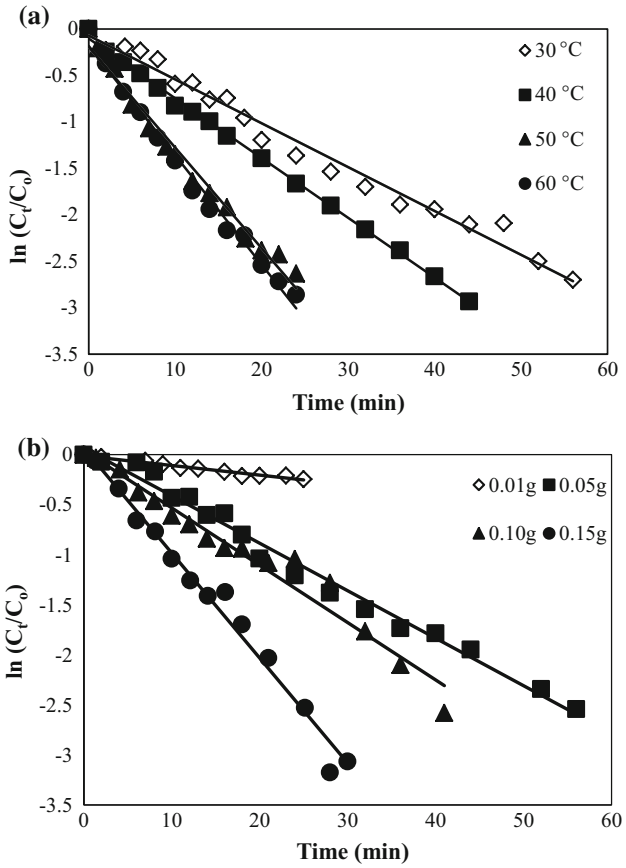

Fig. 4 **a** Plots of ln (C_t/C_o) versus time for the reduction of 4-NP catalyzed by p(AAc)-Co composites at different temperatures and **b** different catalyst amount to show the effect on apparent rate constant. Reaction conditions: 1 mM 4-NP = 50 mL, catalyst = 50 mg (in **a**), $NaBH_4$ = 0.19 g, 250 rpm and 30 °C (in **b**)

of the microgel–cobalt composites were shifted to longer wavelength, i.e., redshifted. The reason for this redshift can be explained by some interactions between cobalt nanoparticles and the functional groups present in the polymeric network. Similar results were observed by Khan et al. (2011) and Feng et al. (1996) where the interaction of Ag NPs with the polymer backbone and coordination of metal cations with nitrogen atoms resulted in a redshift.

Catalytic property

4-NP is more toxic than other nitro compounds (Du et al. 2012). Also, due to an important intermediate step (conversion of 4-NP to 4-AP) in the synthesis of analgesic and antipyretic medicines, it was chosen as model reaction in this work. This reaction does not proceed without aid of any catalyst (Hayakawa et al. 2003). Several nanoparticles were used for reduction of nitro compounds (Butun and Sahiner 2011). In the present work, we used Co nanoparticles entangled in p(AAc) microgel as catalyst for the reduction of 4-NP in the presence of $NaBH_4$. UV–Visible spectrophotometer was used to monitor the progress of reaction. Aqueous solution of 4-NP has an absorption maxima (λ_{max}) at 317 nm; immediately, after addition of $NaBH_4$ the peak undergoes a redshift to λ_{max} = 400 nm as shown in Fig. 3a. This is due to generation of phenolate ion. The phenolate ion has negative charge on oxygen atom which delocalizes on benzene ring and makes it stable. As a result, the negative charge resonates due to conjugation effect and the absorption peak at 400 nm remains fixed with time. A very small decrease in the absorbance was observed even after 4 h of the addition of $NaBH_4$ as shown in Fig. 3a which indicates that 4-NP cannot be reduced without aid of any catalyst. Figure 3b shows the decrease in the absorbance peak at 400 nm and concomitant appearance of a new peak at around 300 nm which indicates the conversion of 4-NP to 4-AP. During this reduction process, the color of reaction mixture changes from bright yellow to colorless (Butun and Sahiner 2011) as can be seen from digital camera images in the inset of Fig. 3b. It is worth mentioning that there appears an isosbestic point around 320 nm as shown in Fig. 3b. The appearance of this isosbestic point suggests that the reduction of 4-NP results in the formation of only 4-AP without side product and also no stable intermediate is produced (Gu et al. 2014).

Since the reduction of 4-NP was carried in 100-fold excess amount of $NaBH_4$, this reaction was assumed to be proceeded by pseudo-first-order kinetics. So pseudo-first-order kinetics was applied to calculate the apparent rate constant (k_{app}). According to pseudo-first-order kinetics equation, $\ln(A_t/A_o)$ was plotted against time where A_o is the absorbance of 4-NP at zero time and A_t represents the absorbance at different time intervals during the course of reaction.

Four different temperatures (30, 40, 50 and 60 °C) were selected to study the effect of temperature on the reduction rate of 4-NP. The rate constant was calculated at each temperature by plotting $\ln(A_t/A_o)$ against time as shown in Fig. 4a. The good linear pattern was observed which confirms that reduction of 4-NP was followed by pseudo-first-order kinetics. The values of k_{app} and coefficients of determination (R^2) for the plots of ln (C_t/C_o) against time obtained at different temperature are given in Table S1. As expected, by increasing the temperature, the k_{app} values were increased. The reason behind the increase in the values of k_{app} for reduction reaction with increase in temperature is that the kinetic energy of reactants is increased with the increase in temperature. This results in more number of effective collisions among reactants. On the other hand, at the same time diffusion rate of molecules into microgel network also increases. Both of these effects collectively increase rate of reaction.

Additionally, the thermodynamic parameters were calculated at different temperatures by using the following well-known Arrhenius (1) and Eyring (2) equations.

$$\ln k = \ln A - (E_a/RT) \quad (1)$$

$$\ln(k/T) = \ln(k_B/h) + \Delta S^{\#}/R - \Delta H^{\#}/R(1/T) \quad (2)$$

where k is the rate constant, A is Arrhenius constant, E_a is the activation energy, R is the real gas constant (8.314 JK^{-1} mol^{-1}), T is the temperature in kelvin, k_B is Boltzmann constant (1.381×10^{-23} JK^{-1}) and h is the Planck's constant (6.626×10^{-34} Js). $\Delta H^{\#}$ and $\Delta S^{\#}$ are activation enthalpy change and activation entropy change.

According to Arrhenius Eq. (1), the activation energy (E_a) for the reduction of 4-NP reduction was calculated from the slope of plot ln k versus $1/T$ and found as 28.288 kJ/mol. $\Delta H^{\#}$ and entropy change $\Delta S^{\#}$ of activated complex were calculated according to Eyring Eq. (2). So $\Delta H^{\#}$ value was calculated from the slope of the plot ln (k/T) versus $1/T$ and found as 24.826 kJ/mol. The positive value of $\Delta H^{\#}$ shows that the formation of activated complex during the reduction of 4-NP is an endothermic process. Also the increase in rate by increasing the temperature indicates that this process is endothermic. The $\Delta S^{\#}$ value was calculated from the intercept of the plot ln (k/T) versus $1/T$ and found to be -188.380 JK^{-1} mol^{-1}. The negative value of $\Delta S^{\#}$ suggests that during this reduction reaction, activated complex was in more ordered form as compared to reactants and the activated complex was formed through association mechanism. This negative value of $\Delta S^{\#}$ also indicates that this reduction reaction was entropically not favorable. However, this opposition against the reduction was overcome by the addition of catalyst which provides a new route for the reaction. Furthermore, the Gibbs free energy was also calculated at every temperature from the following Eq. (3).

$$\Delta G^{\#} = \Delta H^{\#} - T\Delta S^{\#} \quad (3)$$

where $\Delta G^{\#}$ is Gibbs free energy, $\Delta H^{\#}$ is activation enthalpy change and $\Delta S^{\#}$ is activation entropy change while T is the temperature of the reaction medium in Kelvin. The Gibbs free energies were found as 819.051, 837.889, 856.727 and 875.565 kJ/mol at 303, 313, 323 and 333 K, respectively. The positive values at every temperature indicate that the 4-NP reduction reaction was non-spontaneous and it needs an input energy to proceed. This energy was provided by adding catalyst in reaction (Ajmal et al. 2015a, b).

Four different amounts, i.e., 0.01, 0.05, 0.10 and 0.15 g of p(AAc)-Co microgel composite, were used to study the effect of amount of catalyst on the reduction rate of 4-NP. With increase in amount of catalyst, the reduction rate was increased as can be seen from the increasing slopes of plots of $\ln(C_t/C_o)$ against time in Fig. 4b. The reason for such an increase in the reduction rate is that with the increase in amount of catalyst in the reaction mixture the numbers of active sites are increased, and hence, more surface area becomes available for the reactant molecules to come in contact with catalysts which in turn increase the rate of effective collisions and rate of formation of activated complex; hence, rate of reaction is increased.

Another very important feature of a catalyst is its reusability or recycling. It provides information regarding the real application of catalyst system. To investigate reusability, the p(AAc)-Co catalyst used for the reduction of 4-NP was separated from the reaction mixture, washed with DI water and again used as catalyst for the same reaction under the same conditions. In this way, the catalyst was utilized repeatedly for five consecutive cycles. The % conversion of 4-NP and % activity of the catalysts were measured for the reduction of 4-NP which was catalyzed by p(AAc)-Co and are illustrated in Fig. 5. The % conversion was calculated from the difference of absorbance at zero time and at time t, i.e., $A_0 - A_t$, by considering the absorbance at zero time as 100%. On the other hand, % activity was calculated by taking the ratio of every successive cycle's reaction rate to first cycle's reaction rate, i.e., k_1/k_n. It was observed that percent conversion of 4-NP in the first cycle was 92.144% while in the fifth cycle it was 94.568%, so it almost remained unchanged, but the %

activity was increased from 100.00 to 158.034% (about 60% increase). This increase in catalytic activity represents that the catalyst was initially less active, but its activity increased markedly upon reusing. Such an increase can be attributed due to plasticization of the polymer network (Robello et al. 2015). The increase in activity after first cycle may also be due to removal of oxidation layer (metal oxide layer). This oxidation layer might be formed after synthesis which hinders the interaction between the reacting species, i.e., phenolate ions and the catalyst. Removal of impurities from the metal nanoparticle surface is another factor for increase in activity (Wang et al. 2010). Resurfacing/restructuring of microgel composite system also results in increased activity of catalyst (Ajmal et al. 2016; Böhmer et al. 2000). This is because of swelling or transfer of metal nanoparticles from interior part of microgel network to their surface (Robello et al. 2015). The ability of Co nanoparticles containing microgel of being reused without any loss in their catalytic activity represents that Co nanoparticles were strongly entrapped in microgel network and were unable to leave the microgel network. Actually, metal nanoparticles are embedded in meshes of microgel network. In each mesh, metal nanoparticle is surrounded by a net of polymer chains which are woven so strongly that metal nanoparticle cannot diffuse through that. In this way, microgel prevents the loss of Co nanoparticles form microgel and also prevents the reaction medium from contamination of Co nanoparticles.

P(AAc)-Co composite was also used as catalyst for the reduction of methylene blue (MB) in aqueous medium. For this purpose, a 50 mL solution of MB was treated with $NaBH_4$ in the absence and then in the presence of p(AAc)-Co catalyst. It was observed that only 36% of MB solution

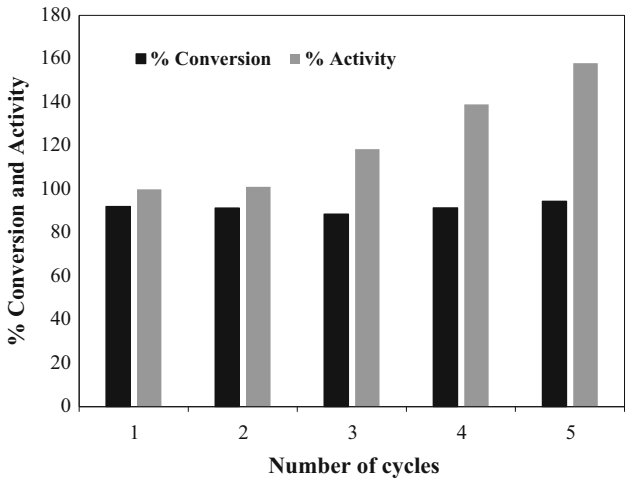

Fig. 5 Change in conversion and activity of p(AAc)-Co catalyst system with repetitive usage. Reaction conditions: 1 mM 4-NP = 50 mL, catalyst = 50 mg, $NaBH_4$ = 0.19 g, 250 rpm and 30 °C

was reduced in 58 min as it is clear from the decrease in absorbance in Fig. S2 (a). On the other hand, 70% decrease in the absorbance was observed in the same time duration when p(MAAc)-Co composite was added in the MB solution along with $NaBH_4$ as shown in Fig. S2 (b) which shows that p(AAc)-Co composite can also act as catalyst for the reduction of MB. It was also observed that p(AAc)-Co composite can also adsorb MB form its aqueous solution. The adsorption of MB p(AAc)-Co composite is depicted in Fig. S2 (c) in terms of decrease in absorbance of MB with the passage of time when p(AAc)-Co composite was present in MB solution.

Adsorption applications

The adsorption ability of pure p(AAc) microgel and p(AAc)-Co microgel composite was investigated by using them as adsorbents in the removal of MB dye from aqueous medium. The maximum amount of dye adsorbed per gram of dried microgel was measured by using the following mass balance equation.

$$q = (C_o - C_e)V/W \quad (4)$$

where q is adsorbed amount (mg/g), C_o is the initial concentration of adsorbate (ppm), C_e is concentration of adsorbate at equilibrium (ppm), V is volume of adsorbate solution (L) and W is mass of adsorbents (mg). The adsorption capacity of the prepared microgel and their composite particles was investigated for the adsorption of MB from aqueous medium. For this study, aqueous solution of MB (1.6×10^{-4} M) was prepared of about 100 mL and 50 mg of p(AAc) microgel particles was used as adsorbent. Adsorption kinetics was studied by withdrawing specific amount of samples from the reaction medium after specific intervals of time. The amount of MB adsorbed on p(AAc) microgel was calculated by measuring the decrease in the concentration of MB solution through UV–visible spectrophotometer. Four different amounts of p(AAc) microgel particles were used to study the effect of adsorbent dose on the % removal of MB from aqueous medium. It was observed that both the rate and % removal were rapidly increased when the adsorbent dose was increased from 12.5 to 100 mg in 100 mL solution of MB as shown in Fig. 6a. It is noteworthy to mention here that our prepared microgel system can adsorb MB up to its maximum capacity in the first 25 min of contact time which shows that this system has potential for the fast removal of MB from water. The rapid increase in adsorption rate can be explained due to increase in available surface area which provides more adsorption sites for adsorption to take place. The total % removal for each amount of adsorbent was greater than 90% as depicted in Fig. 6a.

The initial concentration of dye is also a factor which affects the adsorption capacity of microgels. Therefore, effect of the initial concentration was also studied to

evaluate the adsorption capacity of p(AAc) microgels. To study the effect of the initial concentration of adsorbate solution, MB solution with four different concentrations (2.558, 5.118, 7.676 and 10.235 ppm) was prepared. And in 100 mL of each solution with different concentration, 0.05 g of p(AAc) microgel was added as adsorbent. Aliquots were taken from the reaction mixture after specific time intervals, and after proper dilution the concentration of solution was measured by UV–Vis spectrophotometer. The amount of MB adsorbed on p(AAc) microgels was calculated from the decrease in concentration of solution by applying mass balance equation. The amounts of MB adsorbed on per gram of dried p(AAc) microgels from each solution with the different initial concentration are shown in Fig. 6b. The results indicate that our microgel system can adsorb MB up to its maximum capacity within first 25 min of contact time. Figure 6b shows that with the increase in the initial concentration of MB solution from 2.558 to 10.235 ppm the rate of adsorption was also increased. Also, a large increase from 40 to 200 mg/g in the total adsorbed amount of MB was observed. This increase can occur due to the presence of greater amount of adsorbate following the law of mass action. The results obtained for the adsorption of MB on p(AAc) microgels have been found superior over the earlier reported work. Ayad and El-Nasr (2010) reported adsorption of MB by using polyaniline nanotubes having adsorption capacity of 5 mg/g. Similarly, Zhang and Kong (2011) studied MB removal by applying magnetic nanoparticles Fe_3O_4@C having maximum adsorption capacity of 44.38 mg/g. In addition, the adsorption capacity of activated charcoal that is a commercially available adsorbent for the removal cationic dyes like MB has been found to be equal to 39.09 mg/g (Al-Husseiny 2014). However, in the present study p(AAc) microgels have a much better adsorption capacity of 200 mg/g. So, the p(AAc) microgel composites have immense potential of maximum adsorption as compared to many other adsorbents. Therefore, it can be considered as more effective and suitable adsorbent for the removal of a variety of contaminants along with MB from aquatic medium.

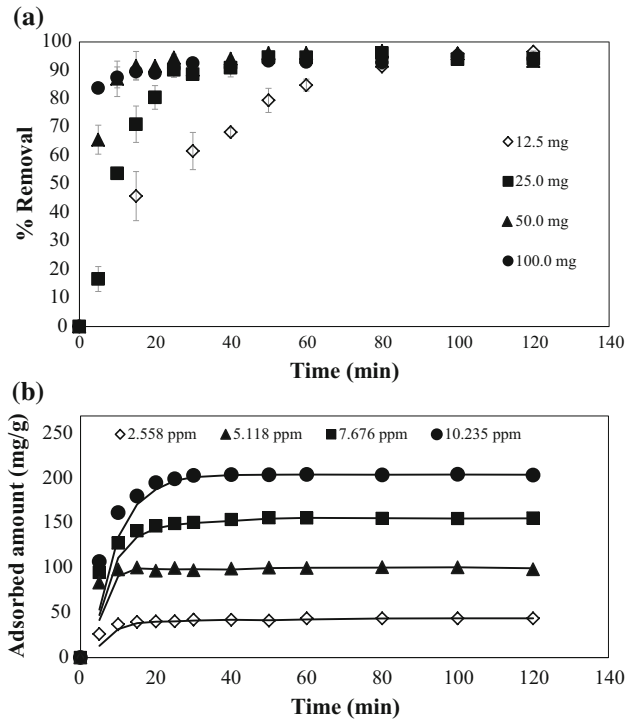

Fig. 6 Plots of **a** % removal of dye MB as a function of time with different amounts of p-(AAc) microgels, [100 mL 1.6×10^{-4} M MB, 50 mg p(AAc) microgels, 400 rpm, room temperature]. **b** Effect of solution concentration on the adsorbed amount of MB on p(AAc) microgels as a function of time [50 mg p(AAc) microgels, 100 mL MB soln., 400 rpm, room temperature]

Adsorption isotherms

There are various ways of adsorption to take place. To determine the way by which adsorption of MB on p(AAc) microgels took place, different adsorption isotherms, i.e., Langmuir, Freundlich and Temkin were constructed. For the adsorption of MB dye, relationship between q_e versus C_e was plotted as shown in Fig. 7a. For the Langmuir adsorption isotherm, the well-known Langmuir Eq. (5) was used

$$C_e/q_e = C_e/q_m + 1/q_m \cdot K_L \quad (5)$$

where C_e is equilibrium concentration of the adsorbate solution (ppm), q_e is the amount of adsorbent adsorbed (mg/g), q_m is the maximum adsorbed amount of adsorbate (mg/g) and K_L is Langmuir constant. Langmuir isotherm was constructed by plotting C_e/q_e versus C_e as presented in Fig. 7b. Langmuir adsorption isotherm did not provide good linear pattern. It reveals that MB did not form monolayer on the surface of p(AAc) microgel particles as assumed by Langmuir adsorption model. Another adsorption isotherm that counts the effect of surface roughness and different types of adsorption sites is Freundlich adsorption isotherm. The mathematical expression of Freundlich adsorption isotherm is given in Eq. 6.

$$\log q_e = 1/n \log C_e + K_F \quad (6)$$

where K_F is adsorption capacity of adsorbent and n is adsorbent intensity for adsorption. The '*1/n*' represents heterogeneity parameter, and its value gives the idea about the favorability and non-favorability of Freundlich isotherm. The values of n in the range of 0.5–10 reveal that adsorption process is favorable. Freundlich adsorption isotherm was constructed by plotting log q_e as a function of log C_e as presented in Fig. 7c. The constants K_F and n were

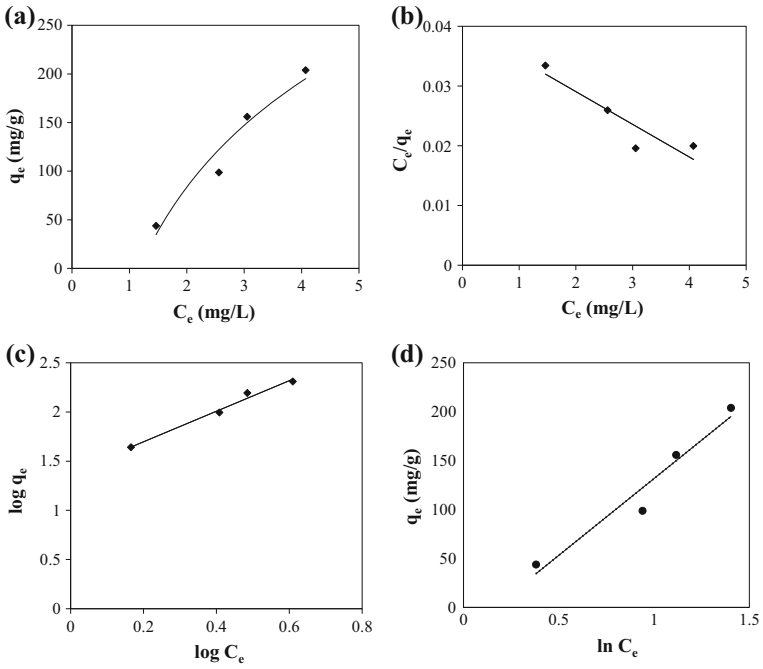

Fig. 7 **a** Plots of q_e versus C_e for the removal of methylene blue (MB) and application of **b** Langmuir adsorption isotherm, **c** Freundlich adsorption isotherm, **d** Temkin adsorption isotherm for the removal of MB

calculated from the intercept and slope, respectively. The correlation coefficient (R^2) is 0.9839 that is very close to 1 and also the value of n greater than 0.5 suggests that adsorption of MB on p(AAc) microgel system was followed by Freundlich isotherm model. As Langmuir and Freundlich isotherms do not consider the possibility of interactions taking place between the adsorbent and adsorbed species, therefore, Temkin isotherm was employed which takes into account the effect of this interaction. Temkin model assumes that free energy of adsorption is involved in adsorbent surface coverage. Mathematical expression for Temkin isotherm is given in Eq. 7.

$$q_e = B \ln K_T + B \ln C_e \quad (7)$$

where K_T is Temkin constant and B is binding energy parameter that can be evaluated from the following relation 8.

$$B = RT/b_T \quad (8)$$

where R is general gas constant, T is temperature in Kelvin and b_T is Temkin isotherm constant. According to Eq. (7), for Temkin isotherm q_e was plotted against ln C_e as shown in Fig. 7d where the constants K_T and B were calculated from the intercept and slope, respectively. The R^2 value of 0.9133 for Temkin adsorption isotherm suggests that this isotherm does not fit on the adsorption data. So it can be concluded that the adsorption of MB on p(AAc) microgels was followed by Freundlich adsorption isotherm.

Kinetic parameters calculated from all the three applied adsorption isotherms for adsorption of MB on p(AAc) microgels are given in Table 1. As indicated from R^2 values, it is clear that that adsorption process was followed by Fruendlich adsorption model.

Adsorption kinetics

Pseudo-first-order and pseudo-second-order kinetic models were applied to evaluate rate constants and order of reaction using the same organic dye MB.

Kinetic parameters calculated for the adsorption of MB from pseudo-first order and pseudo-second order are shown in Table S2. Value of coefficient of determination for pseudo-second-order equation is 0.9997 and very close to 1, and also the q_e value calculated from pseudo-second-order kinetics is 100.00 mg/g which is very close to the experimentally observed value of q_e that is 101.08 mg/g. So, due to more suitable values of correlation coefficient R^2 and the close resemblance of both experimental and theoretical q_e values, it can be concluded that adsorption of MB was carried out by pseudo-second-order kinetics. These results suggest that adsorption process is most probably chemical process (Wu et al. 2009). Furthermore, the rate-limiting step involving ion exchange of sorbent and sorbate might be chemisorption (Ho and Gordon 1999). The adsorptive removal of MB with AAc-based hydrogels form aqueous medium has been studied by Zhou et al. (2011), and Shi et al. (2013) and observed that the adsorption of MB was followed by pseudo-second-order kinetics model (Zhou et al. and Shi et al.). This shows that results obtained in the present work in good agreement with already reported in literature.

Table 1 Kinetic parameters for the adsorption of MB by p(AAc) microgel from the application of Langmuir, Freundlich and Temkin isotherms

Langmuir isotherm constants			Freundlich isotherm constants			Temkin isotherm constants		
K_L (L/g)	q_{max} (mg/g)	R^2	K_F (L/g)	n	R^2	K_T (L/g)	B	R^2
−181.818	−7.273	0.8349	9.636	0.645	0.9839	0.952	138.34	0.9133

Comparison of adsorption on p(AAc) microgels and p(AAc)-Co microgel composites

Adsorption capacity of the prepared magnetic p(AAc)-Co microgel composites was also studied and was compared with the adsorption capacity of p(AAc) microgels. A slight decrease in adsorption capacity for p(AAc)-Co microgel composite was observed as can be seen form plots of adsorbed amount of MB by p(AAc) and p(AAc)-Co particles as function of time in Fig. 8a. The reason for such a decrease in the adsorption capacity is that after in situ fabrication of metal nanoparticles, the empty space inside the microgel network to accommodate the adsorbate is decreased. Another interesting feature of our adsorbent is that they retain their magnetic characteristics even after the adsorption of MB. It was observed that after the adsorption process the microgel particles were freely suspended or settled down in the absence of external magnetic as shown by digital camera image 1 in Fig. 8b. However, as soon as the external magnetic was applied, all the microgel particles were attracted toward the magnet that can be seen by digital camera image 2 in Fig. 8b. This ability of microgel adsorbents to retain their magnetic properties provides an easy, quick and economical way of separating the adsorbent from the adsorption medium.

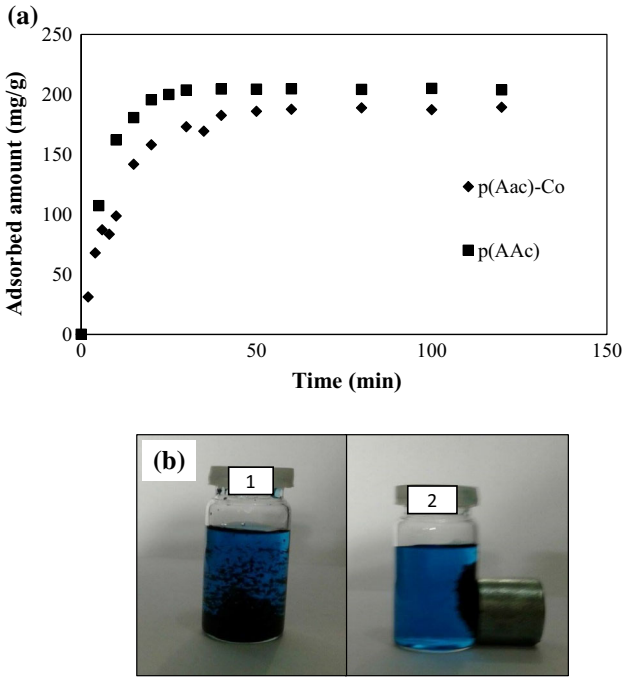

Fig. 8 **a** Plots of adsorbed amount of MB by p(AAc) and p(AAc)-Co particles as function of time (10.255 ppm MB solution = 100 mL, 0.05 g p(AAc) and p(AAc)-Co particles). **b** Digital camera images of p(AAc)-Co composites. (*1*) Suspended in MB in the absence of external magnetic field. (*2*) Attraction of particles toward magnet

Conclusion

Almost monodisperse p(AAc) microgel particles were prepared by inverse suspension polymerization. The prepared microgels were successfully used as microreactors for in situ fabrication of magnetic Co nanoparticles. The prepared p(AAc)-Co microgel composites were found to have excellent catalytic properties for the reduction of 4-NP. The catalytic properties were found to be function of temperature of the reaction medium and an increase in the k_{app} was observed with the increase in temperature. Both the p(AAc) microgel and p(AAc)-Co microgel composites were shown as very good adsorbents for the removal of MB from aqueous medium. A small decrease in the adsorption capacity was observed in case of magnetic p(AAc)-Co microgels, but inherent magnetic behavior provided an easy and effortless way of separation of the adsorbents by the application of external magnetic field. The adsorption speed was observed to be very fast, and p(AAc) microgels were able to adsorb as much as 100 mg of MB per gram of its dried form within 25 min. The Langmuir, Freundlich and Temkin adsorption models were applied on the adsorption data, and Freundlich model was found to be the best fit model for the obtained results. Kinetic models of pseudo-first order and pseudo-second order were also applied, and adsorption of MB was found to abide by pseudo-second order. So in this work we accomplished the synthesis of microgel system with multidimensional applications, i.e., having ability to be used as microreactors for the synthesis of metal nanoparticles, as reaction medium for the reduction of 4-NP and at the same as catalyst for the same reaction and additionally as adsorbent for a toxic industrial dye MB.

Acknowledgements The authors highly acknowledge financial support from Quaid-i-Azam University Islamabad, Pakistan, under University Research Fund 2015.

References

Ahmad T, Rafatullah M, Ghazali A, Sulaiman O, Hashim R, Ahmad A (2010) Removal of pesticides from water and wastewater by different adsorbents: a review. J Environ Sci Heal C 28:231–271

Ajmal M, Siddiq M, Al-Lohedan H, Sahiner N (2014) Highly versatile p (MAc)–M (M: Cu Co, Ni) microgel composite catalyst for individual and simultaneous catalytic reduction of nitro compounds and dyes. RSC Adv 4:59562–59570

Ajmal M, Demirci S, Siddiq M, Aktas N, Sahiner N (2015a) Betaine microgel preparation from 2-(methacryloyloxy) ethyl] dimethyl (3-sulfopropyl) ammonium hydroxide and its use as a catalyst system. Colloid Surf A 486:29–37

Ajmal M, Siddiq M, Aktas N, Sahiner N (2015b) Magnetic Co–Fe bimetallic nanoparticle containing modifiable microgels for the removal of heavy metal ions, organic dyes and herbicides from aqueous media. RSC Adv 5:43873–43884

Ajmal M, Demirci S, Siddiq M, Aktas N, Sahiner N (2016) Simultaneous catalytic degradation/reduction of multiple organic compounds by modifiable p (methacrylic acid-co-acrylonitrile)–M (M: Cu, Co) microgel catalyst composites. New J Chem 40:1485–1496

Al-Husseiny HA (2014) Adsorption of methylene blue dye using low cost adsorbent of sawdust: batch and continues studies. J Babylon Univ/Eng Sci 22:296–310

Ayad MM, El-Nasr AA (2010) Adsorption of cationic dye (methylene blue) from water using polyaniline nanotubes base. J Phys Chem C 114:14377–14383

Böhmer U, Franke F, Morgenschweis K, Bieber T, Reschetilowski W (2000) Enantioselective hydrogenation of ethyl pyruvate: long-term performance of chirally modified Pt/zeolite catalysts. Catal Today 60:167–173

Butun S, Sahiner N (2011) A versatile hydrogel template for metal nano particle preparation and their use in catalysis. Polymer 52:4834–4840

Dai R, Chen J, Lin J, Xiao S, Chen S, Deng Y (2009) Reduction of nitro phenols using nitroreductase from *E. coli* in the presence of NADH. J Hazard Mater 170:141–143

de Santa Maria LC, Amorim MC, Aguiar MR, Guimarães PIC, Costa MA, de Aguiar AP, Rezende PR, de Carvalho MS, Barbosa FG, Andrade JM (2001) Chemical modification of cross-linked resin based on acrylonitrile for anchoring metal ions. React Funct Polym 49:133–143

Du X, He J, Zhu J, Sun L, An S (2012) Ag-deposited silica-coated Fe_3O_4 magnetic nanoparticles catalyzed reduction of p-nitrophenol. Appl Surf Sci 258:2717–2723

Feng Y, Schmidt A, Weiss R (1996) Compatibilization of polymer blends by complexation. 1. Spectroscopic characterization of ion-amide interactions in ionomer/polyamide blends. Macromolecules 29:3909–3917

Gu S, Wunder S, Lu Y, Ballauf M (2014) Kinetic analysis of the catalytic reduction of 4-nitrophenol by metallic nanoparticles. J Phys Chem C 2014(118):18618–18625

Hayakawa K, Yoshimura T, Esumi K (2003) Preparation of gold-dendrimer nanocomposites by laser irradiation and their catalytic reduction of 4-nitrophenol. Langmuir 19:5517–5521

Hernández R, Mijangos C (2009) In situ synthesis of magnetic iron oxide nanoparticles in thermally responsive alginate-poly (N-isopropylacrylamide) semi-interpenetrating polymer networks. Macromol Rapid Commun 30:176–181

Ho Y, Gordon M (1999) Pseudo-second order model for sorption processes. Process Biochem 5:451–465

Khan A, El-Toni AM, Alrokayan S, Alsalhi M, Alhoshan M, Aldwayyan AS (2011) Microwave-assisted synthesis of silver nanoparticles using poly-N-isopropylacrylamide/acrylic acid microgel particles. Colloid Surf A 377:356–360

Mak S-Y, Chen DH (2004) Fast adsorption of methylene blue on polyacrylic acid-bound iron oxide magnetic nanoparticles. Dyes Pigments 61:93–98

Megharaj M, Pearson H, Venkateswarlu K (1991) Toxicity of phenol and three nitrophenols towards growth and metabolic activities of Nostoc linckia, isolated from soil. Arch Environ Contam Toxicol 21:578–584

Ozay O, Ekici S, Baran Y, Aktas N, Sahiner N (2009) Removal of toxic metal ions with magnetic hydrogels. Water Res 43:4403–4411

Ozay O, Ekici S, Baran Y, Kubilay S, Aktas N, Sahiner N (2010) Utilization of magnetic hydrogels in the separation of toxic metal ions from aqueous environment. Desalination 260:57–64

Ozay O, Inger E, Aktas N, Sahiner N (2011) Hydrogen production from ammonia borane via hydrogel template synthesized Cu, Ni, Co composites. Int J Hydrog Energy 36:8209–8216

Robello DR, Mis MR, Nair M (2015) Micron-sized membrane reactors: multicompartment semipermeable polymer particles containing palladium nanoparticles. J Appl Polym Sci 132. doi:10.1002/app.42021

Sahiner N, Ozay H, Ozay O, Aktas N (2010a) A soft hydrogel reactor for cobalt nanoparticle preparation and use in the reduction of nitrophenols. Appl Catal B 101:137–143

Sahiner N, Ozay H, Ozay O, Aktas N (2010b) New catalytic route: hydrogels as templates and reactors for in situ Ni nanoparticle synthesis and usage in the reduction of 2-and 4-nitrophenols. Appl Catal A 385:201–207

Shaoqing Y, Jun H, Jianlong W (2010) Radiation-induced catalytic degradation of p-nitrophenol (PNP) in the presence of TiO2 nanoparticles. Radiat Phys Chem 79:1039–1046

Shi et al (2013) Removal of methylene blue from aqueous solution by sorption on lignocellulose-g-poly(acrylic acid)/montmorillonite three-dimensional cross-linked polymeric network hydrogels. Polym Bull 70:1163–1179

Wang D, Xin HL, Yu Y, Wang H, Rus E, Muller DA, Abruña HD (2010) Pt-decorated PdCo@ Pd/C core–shell nanoparticles with enhanced stability and electrocatalytic activity for the oxygen reduction reaction. J Am Chem Soc 132:17664–17666

Wu Y et al (2009) Adsorption of copper ions and methylene blue in a single and binary system on wheat straw. J Chem Eng Data 12:3229–3234

Yagub MT, Sen TK, Afroze S, Ang HM (2014) Dye and its removal from aqueous solution by adsorption: a review. Adv Colloid Interface Sci 209:172–184

Yang S-T, Chen S, Chang Y, Cao A, Liu Y, Wang H (2011) Removal of methylene blue from aqueous solution by graphene oxide. J Colloid Interface Sci 359:24–29

Zendehdel M, Barati A, Alikhani H, Hekmat A (2010) Removal of methylene blue dye from wastewater by adsorption onto semi-inpenetrating polymer network hydrogels composed of acrylamide and acrylic acid copolymer and polyvinyl alcohol. J Environ Health Sci Eng 7:431–436

Zhang Z, Kong J (2011) Novel magnetic Fe_3O_4@C nanoparticles as adsorbents for removal of organic dyes from aqueous solution. J Hazard Mater 193:325–329

Zhou et al (2011) Removal of methylene blue dyes from wastewater using cellulose-based super adsorbent hydrogels. Polym Eng Sci 51:2417–2424